

Cold and warm dust along a merging galaxy sequence

E. M. Xilouris¹, A. E. Georgakakis¹, A. Misiriotis², V. Charmandaris³

¹ *Institute of Astronomy & Astrophysics, National Observatory of Athens, I. Metaxa & V. Pavlou, Athens, 15236, Greece*

² *University of Crete, Physics Department, PO Box 2208, 71003 Heraklion, Crete, Greece*

³ *Astronomy Department, Cornell University, Ithaca, NY 14853*

6 July 2018

ABSTRACT

We investigate the cold and warm dust properties during galaxy interactions using a merging galaxy sample ordered into a chronological sequence from pre- to post-mergers. Our sample comprises a total of 29 merging systems selected to have far-infrared and sub-millimeter observations. The sub-millimeter data are mainly culled from the literature while for 5 galaxies (NGC 3597, NGC 3690, NGC 6090, NGC 6670 and NGC 7252) the sub-millimeter observations are presented here for the first time. We use the 100–to–850 μm flux density ratio, f_{100}/f_{850} , as a proxy to the mass fraction of the warm and the cold dust in these systems. We find evidence for an increase in f_{100}/f_{850} along the merging sequence from early to advanced mergers and interpret this trend as an increase of the warm relative to the cold dust mass. We argue that the two key parameters affecting the f_{100}/f_{850} flux ratio is the star-formation rate and the dust content of individual systems relative to the stars. Using a sophisticated model for the absorption and re-emission of the stellar UV radiation by dust we show that these parameters can indeed explain both the increase and the observed scatter in the f_{100}/f_{850} along the merging galaxy sequence. We also discuss our results under the hypothesis that elliptical galaxies are formed via disc galaxy mergers.

Key words: ISM: dust, extinction – Infrared: galaxies – Infrared: ISM

1 INTRODUCTION

Early studies on the dust properties of spiral galaxies using IRAS data suggested a gas-to-dust ratio about 5–10 times larger than the Milky Way (Devereux & Young 1990; Sanders et al. 1991). This apparent conflict was interpreted as indirect evidence for the presence of a cold dust component at a temperature $T=15\text{--}25\text{ K}$ heated by the diffuse interstellar radiation field (Cox, Krugel & Mezger 1986; Rowan-Robinson & Crawford 1989). Dust at such low temperatures remains undetected at the IRAS wavebands, that primarily probe warmer dust ($T > 30\text{ K}$), and can only be identified by observations at longer wavelengths ($> 100\mu\text{m}$). It was only recently that the SCUBA bolometer array on the James Clerk Maxwell Telescope (JCMT) has provided sufficient sensitivity at submillimeter (sub-mm) wavelengths (450, 850 μm) to directly confirm the presence of a dominant cold dust component in nearby spirals (Alton et al. 1998a; Alton et al. 1998b; Frayer et al. 1999; Papadopoulos & Seaquist 1999; Dunne et al. 2000; Dunne & Eales 2001).

In more active luminous infrared galaxies (LIGs), with enhanced star-formation or the presence of a central AGN, sub-mm observations also suggest the presence of cold cirrus. Unlike quiescent spirals however, LIGs also show a promi-

nent warm dust component ($T=30\text{--}60\text{ K}$) most likely heated by the starburst (Klaas et al. 2001; Lisenfeld, Issak & Hills 2000). The enhanced activity in LIGs is believed to be triggered by interactions and mergers. It is therefore, interesting to explore the role of such violent events in heating the dust and hence, modifying the relative amounts of the cold and the warm dust component in galaxies. Klaas et al. (2001) have searched for systematic differences in the far-infrared (far-IR) to sub-mm luminosity ratio of interacting and non-interacting LIGs classified on the basis of their optical morphology. Their analysis did not show any trends suggesting either problems with their classification scheme or similar dust temperature distributions in the two sub-samples. Studies of selected interacting galaxies (mostly LIGs) indeed, suggest that cold dust is present in these systems even in the regions experiencing starburst activity where the stellar radiation field heating the dust is most intense (Haas et al. 2000). This may be due to effective shielding of the cold dust component by warmer dust.

In this paper we further explore the issue of dust heating during galaxy encounters by exploiting the large SCUBA database as well as sub-mm observations presented in the literature. Our interacting galaxy sample is compiled from the Georgakakis et al. (2000) study and comprises well sepa-

rated spirals, systems close to nuclear coalescence and young merger remnants. Our sample is larger compared to previous studies and also spans a wider range of interactions stages.

Section 2 discusses our sample selection while Section 3 presents the reduction of the data used in our study. In Section 4 we present our results which are discussed in Section 5. Finally section 6 summarises our conclusions. Throughout this paper we adopt $H_0 = 75 \text{ km s}^{-1} \text{ Mpc}^{-1}$.

2 THE SAMPLE

In this paper we use the interacting galaxy sample presented by Georgakakis et al. (2000) comprising disk galaxy mergers of similar mass. This is culled from a number of studies (Keel & Wu 1995; Gao & Solomo 1999; Gao et al. 1998; Surace et al. 1993) in an attempt to minimize any biases introduced by different selection criteria (e.g. far-IR, morphological selection) used to compile interacting galaxy samples. We note however, that most of the galaxies in that study are far-IR luminous and are also biased against mergers occurring along our line of sight. Therefore, although the Georgakakis et al. (2000) sample is by no means statistically complete, it could be regarded as representative of interacting systems and merger remnants spanning a wide range of properties. The sample employed in this study is presented in Table 1 and comprises only those systems from the Georgakakis et al. (2000) study that have sub-mm data from either the SCUBA archive or the literature.

Following Georgakakis et al. (2000) we use the galaxy ‘age’ parameter providing an estimate of the evolutionary stage of each system relative to the time of the merging of the two nuclei. Such a chronological sequence allow us to explore the evolution of the galaxy properties at different times during the interaction. Negative ‘ages’ are for pre-mergers while positive ‘ages’ correspond to merger remnants. For pre-mergers the ‘age’ is estimated by dividing the projected separation of the two nuclei, δr , by an (arbitrary) orbital decay velocity $v = 30 \text{ km s}^{-1}$. It is clear that the ‘age’ parameter for pre-mergers is affected by projection effects or different interaction geometries. However, to the first approximation, it provides an estimate of the stage of the merging and allows plotting of pre- and post-mergers on the same scale. For post-mergers we adopt the evolutionary sequence defined by Keel & Wu (1995) using dynamical and morphological criteria. In particular, the ‘age’ parameter for these systems is calculated by multiplying the dynamical stage number, defined by Keel & Wu (1995), by the factor $4 \times 10^8 \text{ yr}$. This conversion factor is found to be appropriate for the 3 merger remnants in the Keel & Wu sample with available spectroscopic estimates (i.e. NGC 2865, NGC 3921, NGC 7252; Forbes, Ponman & Brown 1998). It should be stressed that the ‘age’ parameter for both pre- and post-mergers does not represent an absolute galaxy age but is an indicator of the evolutionary stage of the interaction.

3 OBSERVATIONS

In addition to the sub-mm data available in the literature we have analysed unpublished SCUBA archival data for five merging systems in the present sample: NGC 3597,

NGC 3690, NGC 6090, NGC 6670 and NGC 7252. The observations of these galaxies were made with the SCUBA sub-mm bolometer array (Holland et al. 1999) which is mounted on the JCMT and provides simultaneous imaging at 450 and 850 μm for a region of sky of 2.3 arcmin in diameter. SCUBA is an array of 37 bolometers (HPBW=14.7 arcsec) at 850 μm and 91 (HPBW=7.5 arcmin) at 450 μm . In order to provide fully sampled images, the secondary mirror moves in a 64-step jiggle pattern, with the integration time lasting 1 s at each position. After the 16 steps of jiggle pattern, the telescope nods in order to allow for slowly varying sky gradients. For NGC 3597 (observed in 5-Apr-2000), NGC 3690 (observed in 24-Nov-98), NGC 6670 (observed in 5, 6-Nov-97) and NGC 7252 (observed in 5-Jul-97) the chop throw was 120, 80, 80 and 120 arcsec respectively. For NGC 6090 a chop throw of 120, 80 and 60 arcsec was used during the observing runs of 12-Mar-1998, 5-Dec-1997 and 4-Jan-2000 respectively. All observations were made with grade-1 weather ($\tau_{225} < 0.05$) except for 5-Apr-2000 and 4-Jan-2000 where weather conditions were of grade-3 ($\tau_{225} \sim 0.1$).

The data were reduced using the SURF software package (Jenness et al. 1997). We made corrections for the atmospheric absorption using the opacities derived from skydip measurements taken regularly every night. Noisy bolometers were flagged and large spikes were removed. During each night, several calibration sources were mapped in order to flux calibrate our images. The SCUBA beams have moderate error lobes and since all our targets are extended sources, we corrected the calibration in order to account of emission outside the central beam. We estimated the flux loss due to the secondary lobes by evaluating the average peak-to-aperture flux ratios measured for the calibration sources for each observing night. All five new galaxy systems presented in this work were detected at 850 μm while only NGC 3690 showed significant signal in the 450 μm band. For all our observations we estimated a calibration uncertainty (based on differences among the nightly calibration values) which are reported in Table 1. The 850 μm emission of these galaxies is presented in Figure 1 with contours overlaid on top of the optical DSS images. Unfortunately, the relatively large beam size of SCUBA ($\sim 4 \text{ kpc}$ at a distance of 50 Mpc) does not allow for a morphological study of these systems. We note however, that some of these systems (mostly early pre-mergers) have 850 μm emission that shows two peaks, while others (the more evolved systems) show a single peak.

4 RESULTS

The dust properties of our sample are quantified using the 100-to-850 μm flux density ratio, f_{100}/f_{850} . This provides an estimate of the relative mass fraction of the warm and the cold dust component. Indeed, the sub-mm wavelengths (e.g. 450 and 850 μm) are sensitive to cold dust ($T \approx 15 - 25 \text{ K}$; Alton et al. 1998a; Alton et al. 1998b; Bianchi et al. 1998; Dunne et al. 2000; Dunne & Eales 2001) while the 100 μm flux density primarily probes the warmer dust ($T \approx 35 \text{ K}$) heated by the star-formation activity (Devereux & Young 1990; Devereux et al. 1994; Klaas et al. 2001; Misiriotis et al. 2004). Also the presence of an AGN in some of our systems does not affect our results. This is because at the wavelengths used in this study the contamination of the ob-

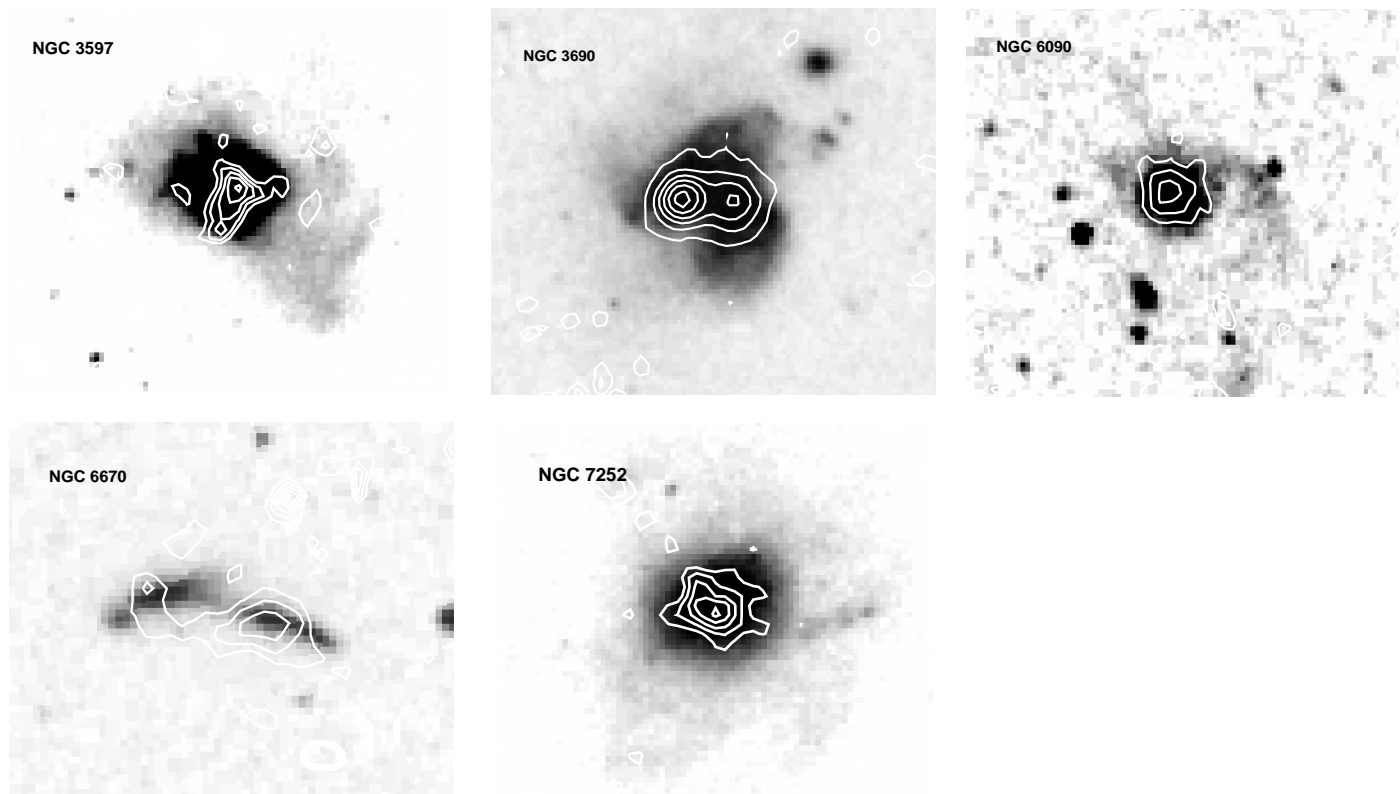


Figure 1. Sub-mm images of NGC 3597, NGC 3690, NGC 6090, NGC 6670 and NGC 7252. Contour levels are 0.020, 0.033, 0.047, 0.060, 0.073 Jy/beam for NGC 3597; 0.030, 0.068, 0.107, 0.146, 0.184, 0.222 Jy/beam for NGC 3690; 0.020, 0.051, 0.082 Jy/beam for NGC 6090; 0.040, 0.063, 0.086 Jy/beam for NGC 6670 and 0.010, 0.017, 0.025, 0.032, 0.040 Jy/beam for NGC 7252.

served fluxes due to AGN emission is expected to be small (e.g. Della Ceca et al. 2002; Zezas, Ward & Murray 2003). This is also discussed below.

We further explore the connection between f_{100}/f_{850} and the dust content by estimating the warm (M_W) and the cold (M_C) dust mass of our sample galaxies and then plotting f_{100}/f_{850} against the ratio M_C/M_W . The M_W , M_C are calculated by fitting two modified Planck functions, each with different temperature, to the observed far-IR to sub-mm spectral energy distribution of our sources. We follow the method described by Dunne & Eales (2001) keeping the dust emissivity index fixed to $\beta = 2$. In this exercise we combine the IRAS and the SCUBA data presented in Table 1 with the flux density measurements at other far-IR and sub-mm wavelengths from the literature. Only systems with data in at least four wavelengths, of which at least two should lie in the sub-mm regime, are fitted.

The emission at a particular wavelength is modeled by a two-temperature graybody described by

$$F_\lambda = \frac{N_W}{\lambda^\beta} B(\lambda, T_W) + \frac{N_C}{\lambda^\beta} B(\lambda, T_C), \quad (1)$$

where T_W and T_C are the temperatures of the warm and the cold dust component respectively and β is the dust emissivity index, fixed to $\beta = 2$ for consistency with the study of Dunne & Eales 2001. N_W and N_C are normalization constants that determine the mass of each of the warm and cold components respectively. As already argued in Alton et al. (1998a), although the dust masses that are calculated with this technique are not very accurate (due to

the adopted dust properties), the cold-to-warm dust mass ratio M_C/M_W (which is equivalent to N_C/N_W) provides a more secure estimate of the relative content of warm and cold dust within the galaxies. We also estimate the statistical error of the M_C/M_W ratio due to the uncertainty in the measured fluxes using the bootstrap method described by Dune & Eales (2001). For each galaxy in our sample mock SEDs were constructed by randomising the fluxes at each wavelength, assuming that they follow a Gaussian distribution with mean the measured flux and standard deviation the uncertainty estimated from the observations. A total of 100 mock SEDs were produced for individual galaxies in our sample and each of them was then fitted with two modified black bodies in the same way as with the real data. The standard deviation of M_C/M_W ratio from the 100 trials provides an estimate of the uncertainty in this parameter. We note however, that this uncertainty does include systematic biases that may affect the M_C/M_W ratio. For example, the sparse wavelength coverage, uncertainties in the opacity coefficients κ_d and the emissivity index β as well as degeneracies in the fitting parameters make the decomposition of the observed SED into two blackbodies not unique (Klaas et al. 2001).

The results of the fits are presented in Table 2. Figure 2 plots f_{100}/f_{850} against the ratio M_C/M_W for the merging galaxies presented in this study (solid circles) and the galaxies presented in Dunne & Eales 2001 (open circles). Despite the large scatter there is evidence for a correlation in the sense that sources with a lower cold-to-warm dust mass

Table 1. Observational information of the galaxies.

Name	age ($\times 10^8$ yr)	D (Mpc)	f_{60} (Jy)	f_{100} (Jy)	f_{850} (Jy)	λ (μm)	f_λ (Jy)	Refs.
ARP 220	+0.0	83.6	103.33	113.95	0.832 ± 0.086	350, 450, 800 1100, 1250, 1300	11.7, 3.0, 0.83 0.35, 0.23, 0.02	f, c, c f, d, a
ARP 240	-11.2	90.6	10.68	18.69	0.283 ± 0.039			
ARP 271	-8.0	34.9	9.93	24.81	0.548 ± 0.086			
ARP 302	-8.8	134.7	6.68	14.54	0.215 ± 0.031	450, 1100	0.37, 0.04	e, e
ARP 90	-1.9	33.2	9.14	13.69	0.119 ± 0.022			
ARP 91	-1.9	28.8	11.55	19.50	0.306 ± 0.031			
IC 1623	-2.0	80.2	22.19	30.32	0.273 ± 0.038	450	2.43	h
IC 883	-0.1	93.3	13.69	24.90	0.104 ± 0.016	350, 750	1.95, 0.20	j, j
IRAS 01418+1651	-1.4	109.7	11.86	13.75	0.076 ± 0.015			
IRAS 03359+1523	-2.2	141.5	5.77	6.53	0.044 ± 0.009			
MRK 848	-1.6	160.7	9.15	10.04	0.060 ± 0.014	450	0.42	j
MRK 273	-0.2	151.0	27.45	22.44	0.104 ± 0.010	350, 450, 800 1100, 1300	1.0, 0.71, 0.08 0.05, 0.02	f, f, f f, b
NGC 1614	-0.7	63.7	33.12	36.19	0.219 ± 0.032	350, 450	1.87, 0.98	g, j
NGC 2623	+1.6	73.8	25.72	27.36	0.091 ± 0.014	350, 750	2.25, 0.17	g, j
NGC 3597	-0.3	46.5	12.71	15.96	0.061 ± 0.006			
NGC 3690	-1.4	40.6	121.64	122.45	0.486 ± 0.049	350, 450, 1250	7.50, 1.50, 0.10	a, l, d
NGC 4038/4039	-2.5	21.9	48.68	82.04	0.760 ± 0.076	450	4.08	i
NGC 4194	+0.8	33.4	25.66	26.21	0.113 ± 0.220	350, 1300	0.97, 0.01	g, b
NGC 4922	-3.7	98.1	6.20	7.30	0.053 ± 0.012			
NGC 520	-1.9	30.4	31.55	46.56	0.325 ± 0.050	350	4.89	g
NGC 5256	-1.6	111.4	9.72	10.35	0.082 ± 0.017	1300	0.01	b
NGC 6052	-0.5	62.9	6.46	10.18	0.095 ± 0.015	450	0.72	j
NGC 6090	-1.3	117.0	6.25	9.34	0.103 ± 0.010	150, 200	8.67, 4.48	m, m
NGC 6240	-0.3	97.9	32.22	22.71	0.155 ± 0.045	450	1.07	k
NGC 6670	-4.9	63.7	8.24	15.18	0.137 ± 0.014	180, 200	14.5, 13.5	n, n
NGC 7252	+2.4	62.5	4.28	7.73	0.045 ± 0.005	1250	0.025	o
NGC 7592	-1.9	97.7	9.30	10.50	0.108 ± 0.019	150, 180, 200	6.4, 5.8, 4.6	p, p, p
UGC 2369	-4.3	124.7	8.14	11.10	0.072 ± 0.013	450	0.52	j
UGC 4881	-3.5	157.1	6.53	10.21	0.065 ± 0.013			

a: Chini et al. 1986; b: Kruegel et al. 1988; c: Eales, Wynn-Williams & Duncan 1989; d: Carico et al. 1992;

e: Clements, Andreani & Chase 1993; f: Rigopoulou, Lawrence & Rowan-Robinson 1996; g: Benford et al. 1999; h: Frayer et al. 1999;

i: Haas et al. 2000; j: Dunne & Eales 2001; k: Klaas et al. 2001; l: this work.; m: Calzetti et al. 2000; n: Spinoglio, Andreani & Malkan 2002;

o: Andreani & Franceschini 1996; p: Siebenmorgen, Krugel & Chini 1999

fraction (low M_C/M_W values) also have enhanced f_{100}/f_{850} flux density ratio. The Spearman's rank correlation test rejects the null hypothesis that the f_{100}/f_{850} and the M_C/M_W are uncorrelated with a probability 0.015 corresponding to $\approx 2.5\sigma$. Similar conclusions are obtained if we use the larger sample of Dunne & Eales (2001) that comprise both interacting systems and isolated galaxies.

The large scatter in Figure 2 may be intrinsic suggesting that parameters other than M_C/M_W may affect the f_{100}/f_{850} . However, the systematics discussed above may also bias the M_C/M_W ratio and contribute to the observed scatter. We avoid the above systematics by using observables to describe the dust properties (e.g. f_{100}/f_{850}) rather than parameters derived from spectral fittings.

Figure 3 plots the ratio f_{100}/f_{850} as a function of the age parameter. As explained in Section 2, negative ages correspond to pre-merger stages, zero is for the nuclear coalescence while positive ages are for merger remnants. In Figure 3 there is evidence for an increase in the f_{100}/f_{850} ratio as the interaction progresses toward the final stages of the merger. We estimate a Spearman rank correlation coefficient $r = 0.64$ and a probability that there is no correlation $P = 0.07$ per cent. Therefore, the null hypothesis that the

f_{100}/f_{850} and the age parameter are uncorrelated can be rejected at the $\approx 3.5\sigma$ confidence level.

We note that this statistically significant correlation is not due to f_{100} or f_{850} being individually correlated with the age parameter. We normalise f_{100} and f_{850} with the K -band flux (f_K) of our systems from the Two Micron All Sky Survey (2MASS; Jarrett et al. 2000). Using the Spearman rank correlation test we find that the probability that the age parameter is uncorrelated with f_{100}/f_K and f_{850}/f_K of 4 ($\approx 2\sigma$) and 28 ($\approx 1\sigma$) per cent respectively. Therefore, the null hypothesis that there is no correlation between these parameters cannot be rejected at a high confidence level. Also, the trend between f_{100}/f_{850} and the age parameter is not affected by the presence of an AGN in some of our sample galaxies. This is demonstrated in Figure 3 where systems identified as AGN in the catalogue of Veron-Cetty & Veron (2003) are plotted with crossed circles. The AGNs in that figure follow a similar trend to the remaining systems.

The mean f_{100}/f_{850} ratio of isolated spirals from the sample of Misiriotis et al. (2004) is also plotted in Figure 3 at an arbitrary age of -13. Based on the discussion above this trend can be interpreted as an increase of the warm relative to the cold dust mass from isolated spirals and early

Table 2. Dust temperatures and cold-to-warm dust mass ratio derived by fitting a two-temperature graybody curve with $\beta = 2$. The uncertainty of the cold-to-warm dust mass ratio is given in the last column.

Name	T_W (K)	T_C (K)	M_C/M_W	$\sigma_{(M_C/M_W)}$
ARP 220	49.3	22.8	39.7	10.4
ARP 302	40.9	20.1	87.4	13.6
IC 1623	55.6	23.1	132.4	8.9
IC 883	43.2	17.0	12.7	2.5
MRK 848	35.5	11.7	11.1	2.5
MRK 273	50.4	27.4	14.1	5.2
NGC 1614	38.7	23.1	1.8	0.9
NGC 2623	48.4	26.2	17.8	1.8
NGC 3690	36.8	36.7	7.6	0.4
NGC 4038/4039	21.4	28.6	55.4	9.7
NGC 4194	36.5	36.5	0.87	1.1
NGC 520	52.2	25.1	71.2	3.2
NGC 5256	48.4	23.1	46.7	18.7
NGC 6052	34.7	19.3	16.1	2.3
NGC 6090	32.3	14.7	11.2	2.0
NGC 6240	51.8	22.2	50.3	14.7
NGC 6670	30.9	14.2	34.4	6.0
NGC 7252	34.9	22.3	8.9	1.2
NGC 7592	33.6	14.2	23.1	2.9
UGC 2369	34.3	18.9	4.4	2.0

interacting systems to advanced mergers. Such a transition of the cold dust to warmer temperatures can be attributed to heating by the more intense UV radiation field of the enhanced star-formation triggered by the merging (e.g. Casoli et al. 1991; Keel & Wu 1995; Georgakakis et al. 2000). However, the lack of a statistically significant correlation between f_{100}/f_K ($\approx 2\sigma$; providing an estimate of the SFR normalised to the total galaxy mass) and age suggests that parameters other than the SFR also play an important role in moderating the f_{100}/f_{850} ratio.

We further explore this using the sophisticated model of Misiriotis et al. (2004) for the absorption of the UV/optical radiation by dust and its re-emission at far-IR and sub-mm wavelengths. This model produces UV to sub-mm SEDs for a given input system geometry, stellar population (e.g. young and old stars), dust content and total galaxy mass. Our goal is not to derive physical parameters for the individual interacting systems but to show that this model, under simple assumptions, can reproduce the observed f_{100}/f_{850} range of our sample.

The interacting galaxies studied here clearly have complex morphology that is difficult to quantify and to model. To the first approximation we assume simple exponential disk-galaxy geometry. Although clearly a more complex geometry is required for each one of our interacting systems, this is an approximation that allows some insight into how different parameters (e.g. star-formation rate, dust content) affect the f_{100}/f_{850} ratio. Since we do not attempt to model individual systems the exact geometry of the interaction is not a crucial parameter for this study. The total mass of the model galaxy is parametrised by its K -band luminosity. We adopt $M_K = -24.5$ mag, the mean absolute magnitude of our sample galaxies. The dust mass of the fiducial galaxy is assumed to be in the range $\approx 10^7 - 10^8 M_\odot$, similar to the dust masses estimated using the simple black-body fits de-

scribed above. The stellar content is directly associated with the density of the UV radiation responsible for the heating of the dust and is parametrised by the star-formation rate. Here we use three different values for the star-formation rate SFR=1, 10 and $60 M_\odot$. For a given SFR and dust mass (in the range $\approx 10^7 - 10^8 M_\odot$) we derive the f_{100}/f_{850} ratio predicted by the Misiriotis et al. (2004) model. The shaded regions in Figure 3 represent the f_{100}/f_{850} for different SFRs. The lower and upper boundaries of these regions correspond to dust masses of 10^7 and $10^8 M_\odot$ respectively. Clearly, both the SFR and the total dust mass (relative to the stellar mass) are important for the f_{100}/f_{850} ratio.

As expected the model predicts that higher star-formation rates heat the dust resulting in higher f_{100}/f_{850} ratios. Indeed, the model of Misiriotis et al. (2004) predicts an increase in the mean (weighted by mass) dust temperature of the cold component for different SFRs: we find that for SFR=1 M_\odot /yr the dust temperature is between 16 and 18 K, for 10 M_\odot /yr it is between 19 and 22 K while for SFR=60 M_\odot /yr it is between 24 and 28 K.

Also, keeping the SFR fixed, more dusty systems have lower f_{100}/f_{850} which can be attributed to higher fraction of UV/optical photons absorbed by the dust, heating it to temperatures $T \lesssim 30$ K and then being re-emitted primarily at sub-mm wavelengths (e.g. $850\mu\text{m}$). For example in the case of the Misiriotis et al. (2004) study, the fraction of UV/optical photons absorbed by the diffuse dust component in individual systems in their sample (as predicted by their best fit model) is anti-correlated with the observed f_{100}/f_{850} at the 2.5σ confidence level. This may also partly explain the scatter seen in Figure 3 since the relative fraction of the warm-to-cold dust for a given SFR varies substantially with dust content. Other factors such as projection effects, differences in the details of individual interactions (e.g. geometry, initial conditions, bulge-to-disk ratio) may also contribute to the scatter in Figure 3. We also note that the diffuse UV/optical radiation field does not have a large impact on the $100\mu\text{m}$ emission, which is primarily dominated by starburst activity taking place in localised galaxy regions.

At post-merger stages the evolution of f_{100}/f_{850} with age after the merging event remains poorly constrained since only 3 systems have SCUBA measurements available. This is also a problem for evolved ellipticals, the alleged product of disc galaxy mergers, with dust properties (e.g. temperature, content) that remain largely unknown. This is mainly because these systems are believed to have very little if any dust and hence are difficult to detect at far-IR and sub-mm wavelengths. Previous observations of ellipticals at sub-mm wavelengths targeted far-IR luminous and optically peculiar systems to maximize the probability of detection (e.g. Fich & Hodge 1993; Wiklind & Henkel 1995; Leeuw et al. 2004). As a result the f_{100}/f_{850} ratios of these systems may not be representative of ellipticals. We attempt to constrain the f_{100}/f_{850} ratio of evolved ellipticals using the sample of Temi et al. (2003). These authors use ISO observations to constrain the far-IR (60–200 μm) SEDs of early type galaxies (not selected on the basis of their far-IR luminosity) and to estimate their warm and cold dust content using methods similar to those outlined here (e.g. modified black-body fittings). Although their results are somewhat uncertain due to the lack of sub-mm observations which are critical as a

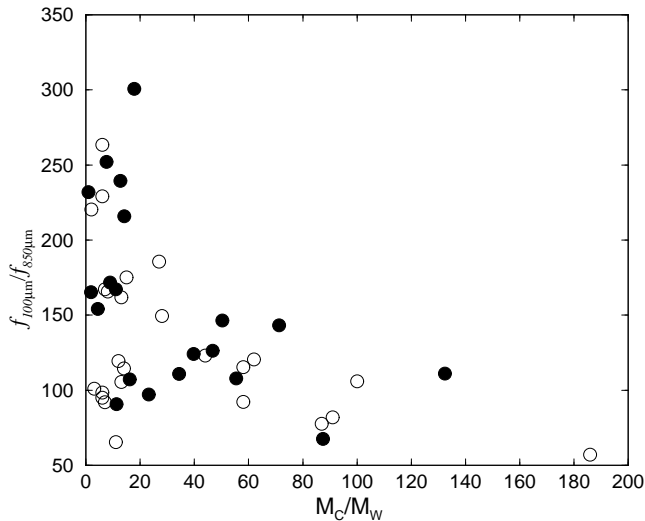


Figure 2. f_{100}/f_{850} flux ratio against the cold-to-warm dust content. The filled circles are the interacting systems in the present sample while the open circles are the galaxies presented in Dunne & Eales (2001).

probe of the cold dust, this study provides the only constraints on the dust properties of early type systems using data extending beyond $100\mu\text{m}$. Using the best fit model of Temi et al. (2003) we extrapolate their observed SEDs to $850\mu\text{m}$ and estimate the mean f_{100}/f_{850} flux density ratio for the elliptical galaxies in their sample. This mean value (54 ± 33) is plotted in Figure 3 (the star arbitrarily plotted at an age of $+5$) and should be considered with caution since the f_{850} flux density is not directly observed. Nevertheless, taken at face value it suggests that the ratio f_{100}/f_{850} in evolved ellipticals is about 1 dex lower compared to young merger remnants. This can be interpreted as dust cooling after the merger event under the hypothesis that elliptical galaxies are formed via disc galaxy mergers. We caution the reader however, that other mechanisms such as spattering of dust grains by X-ray radiation as well as the dispersal of dust in star formation may also affect the f_{100}/f_{850} ratio. Observations at sub-mm wavelengths of elliptical galaxies and post-mergers are essential to further explore different scenarios.

5 DISCUSSION

In this paper we use an interacting galaxy sample ordered into a chronological merging sequence to explore dust properties during gravitational galaxy encounters. We find evidence for an increase in the flux density ratio f_{100}/f_{850} from isolated spirals and early interacting systems to intermediate and late stage mergers close to nuclear coalescence. We interpreted this trend as an increase of the warm relative to the cold dust mass. Both the star-formation triggered by the merging and the dust content of individual systems are important parameters for modifying the f_{100}/f_{850} ratio and the observed trend along the merging galaxy sequence.

Klaas et al. (2001) have also investigated the far-IR to sub-mm properties of luminous infrared galaxies and have searched for systematic differences between isolated and in-

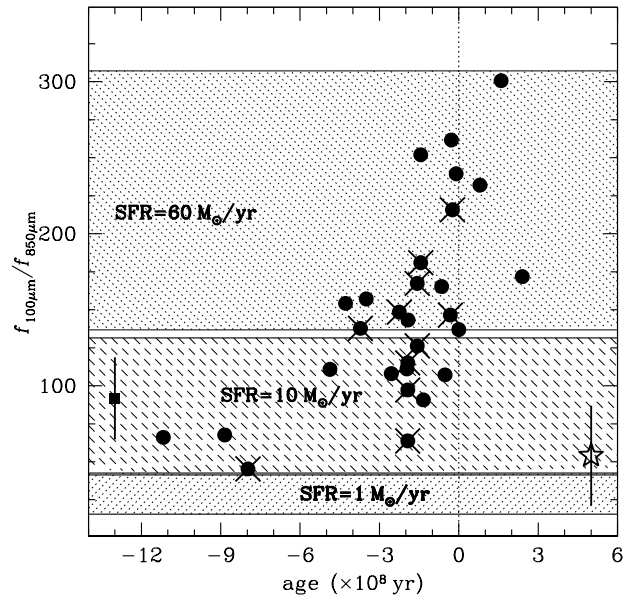


Figure 3. f_{100}/f_{850} flux ratio against the age parameter for our sample of interacting galaxies. The filled circles are the interacting galaxy sample in this study. A cross on top of symbol signifies an AGN in the catalogue of Veron-Cetty & Veron (2003). The square corresponds to the mean f_{100}/f_{850} of isolated spirals from the sample of Misiriotis et al. (2004) arbitrarily plotted at an age parameter of -13 . The star is the mean f_{100}/f_{850} of ellipticals from the sample of Temi et al. (2003; see text for details) arbitrarily plotted at an age parameter of $+5$.

teracting systems classified on the basis of their optical morphology. Unlike our results they find no differences in the relative amounts of warm and cold dust between the two samples. However, these authors do not attempt to order their interacting systems on the basis of the angular separation between the two nuclei (i.e. the age parameter). Also, their sample spans a small range in bolometric luminosity and therefore well separated early interacting systems may be underrepresented.

Dunne & Eales (2001) have performed the most extensive study of the sub-mm dust properties of nearby galaxies to date using the SCUBA bolometer array at the JCMT. They find that in quiescent spirals most of the warm dust ($T > 30\text{K}$) is concentrated in nuclear regions with the cold dust component ($T = 15 - 20\text{K}$) dominating the outer disc. The situation is strikingly different in starbursts where they find that the warm dust region is more extended and therefore dominates the SED. This is attributed to the more intense interstellar radiation field in actively star-forming galaxies. Although Dunne & Eales (2001) do not discuss possible differences in the sub-mm properties between interacting and isolated galaxies in their sample, most of our interacting/merging systems, particularly the more advanced ones, are in a starburst phase. Therefore, on the basis of the Dunne & Eales (2001) findings, for these galaxies we would expect a significant warm dust component compared to isolated (on average more quiescent) spirals.

We note however, that the evidence above does not suggest the absence of cold dust in interacting starbursts.

Indeed, detailed study of selected systems (e.g. ARP 220, NGC 4038/4039) shows significant amounts of cold dust that may dominate the total dust content (Klaas et al. 1997; Haas et al. 2000; Klaas et al. 2001; Dumke, Krause & Wielebinski 2003). Dunne & Eales (2001) argue that the most active starburst activity is usually taking place in well-shielded dust enshrouded regions allowing the presence of very cold dust at the same regions.

Moreover, using our interacting galaxy sample we attempt to explore possible connections between the dust properties of isolated spirals, mergers and evolved ellipticals. This is particularly important in the light of the merger hypothesis postulating that ellipticals are the product of disc galaxy mergers. However, our sample comprises only a few post merger remnants while the cold and warm dust properties of evolved ellipticals remain poorly constrained. Nevertheless, the tentative result of our study is that young merger remnants have f_{100}/f_{850} ratios about 1 dex higher than evolved ellipticals. This may suggest that the dust cools with time after nuclear coalescence, although other scenarios can also explain the lower f_{100}/f_{850} ratios in these systems. Future observations using sensitive instruments such as ALMA and the *Spitzer* satellite will allow us to probe the largely unexplored far-IR to sub-mm regime of early type galaxies. These data have the potential to accurately characterize, for the first time, the dust properties of ellipticals and merger remnants and to search for possible evolutionary effects between these systems.

6 CONCLUSIONS

In this paper we explore the cold and warm dust properties of galaxies during gravitational encounters using a merging galaxy sample ordered into a time sequence and comprising well separated spirals, systems close to nuclear coalescence and young merger remnants. We use the 100 to 850 μm flux density ratio, f_{100}/f_{850} , as a proxy to the mass fraction of the warm and the cold dust in these systems. We find evidence for an increase in f_{100}/f_{850} along the merging sequence from isolated spirals and early interacting systems to advanced mergers. We interpret this trend as an increase of the warm relative to the cold dust mass and argue that the star-formation and the dust content of individual systems are important for modifying the f_{100}/f_{850} ratio.

7 ACKNOWLEDGMENTS

We thank the referee, L. Dunne, for useful comments and suggestions that significantly improved this paper. AG acknowledges funding by the European Union and the Greek Ministry of Development in the framework of the Programme ‘Competitiveness-Promotion of Excellence in Technological Development and Research-Action 3.3.1’, Project ‘X-ray Astrophysics with ESA’s mission XMM’, MIS-64564.

REFERENCES

Alton P.B., Bianchi S., Rand R.J., Xilouris E.M., Davies J.I., Trewhella M., 1998a, ApJ, 507, 125

- Alton P.B., Trewhella M., Davies J.I., et al., 1998b, A&A, 335, 807
- Andreani P., Franceschini A., 1996, MNRAS, 283, 85
- Benford D.J., Cox P., Omont A., Phillips T.G., McMahon, R.G., 1999, ApJ, 518, 65
- Bianchi S., Alton P.B., Davies J.I., Trewhella M., 1998, MNRAS, 298, 49
- Calzetti D., et al., 2000, ApJ, 533, 682
- Carico D.P., Keene J., Soifer B.T., Neugebauer G., 1992, PASP, 10
- Casoli F., Dupraz C., Combes F., Kazes I., 1991, A&A, 251, 32
- Chini R., Kreysa E., Kruegel E., Mezger P.G., 1986, A&A, 166, 8
- Clements D.L., Andreani P., Chase S.T., 1993, MNRAS, 261, 299
- Cox, P. Kruegel, E. Mezger P.G., 1986, A&A, 155, 380
- Della Ceca et al., 2002, ApJ, 581, 9
- Devereux N.A., Young J.S., 1990, ApJ, 359, 42
- Devereux N.A., Price R., Wells L.A., Duric N., 1994, AJ, 108, 1667
- Dumke M., Krause M., Wielebinski R., 2004, A&A, 414, 475
- Dunne L., Eales S.A., 2001, MNRAS, 327, 697
- Dunne L., Eales S.A., Edmunds M., Ivison R., Alexander P., Clements D.L., 2000, MNRAS, 315, 115
- Eales S.A., Wynn-Williams C.G., Duncan W.D., 1989, ApJ, 339, 859
- Frayser D.T., Ivison R.J., Smail I., Yun M.S., Armus L., 1999, AJ, 118, 139
- Gao Y. Solomon P. M., 1999, ApJ, 512, 99
- Gao Y. Gruendl R. A., Hwang C.Y., Lo K.Y., preprint, (astro-ph/9812459)
- Georgakakis A., Forbes D.A., Norris R.P., 2000, MNRAS, 318, 124
- Haas M., Klaas U., Coulson I., Thommes E., Xu C., 2000, A&A, 356, 83
- Holland W., Robson E., Gear W., et al., MNRAS, 303, 659
- Jarrett T.H., Chester T., Cutri R., Schneider S., Skrutskie M., Huchra J.P., 2000, AJ, 119, 2498
- Jenness T., et al., 1997, Starlink User Note 216.1
- Fich M., Hodge P., 1993, ApJ, 415, 75
- Forbes D.A., Ponman T.J., Brown R.J.N., 1998, 508, L43
- Keel W.C., Wu W., 1995, AJ, 110, 129
- Klaas U., et al., 2001, A&A, 379, 823
- Klaas U., Haas M., Heinrichsen I., Schulz B., 1997, A&A, 325, 21
- Kruegel E., Chini R., Kreysa E., Sherwood W.A., 1988, A&A, 190, 47
- Leeuw L. L., Sansom A. E., Robson E. I., Haas M., Kuno N., 2004, ApJ, accepted, astro-ph/0406011
- Lisenfeld U., Isaak K.G., Hills R., 2000, MNRAS, 312, 433
- Misiriotis A., Papadakis I.E., Kylafis N.D., Papamastorakis J., 2004, A&A, 417, 39
- Papadopoulos P., Seaquist E.R., 1999, ApJ, 514, 95
- Rigopoulou D., Lawrence, A., Rowan-Robinson M., 1996, MNRAS, 278, 1049
- Rowan-Robinson M., Crawford J., 1989, MNRAS, 238, 523
- Sanders D.B., Scoville N.Z., Soifer B.T., 1991, ApJ, 370, 158
- Siebenmorgen R., Krgel E., Chini R., 1999, A&A, 351, 495
- Spinoglio L., Andreani P., Malkan M., 2002, ApJ, 572, 105
- Surace J.A., Mazzarella J., Soifer B.T., Wehrle A.E., 1993, AJ, 105, 864
- Temple P., Brighenti F., Mathews W.G., Bregman J.D., 2004, ApJS, 151, 237
- Veron-Cetty M.P., Veron P., 2003, A&A, 412, 399
- Wiklind T. & Henkel C., 1995, A&A, 297, L71
- Zezas A., Ward M.J., Murray S.S., 2003, ApJ, 594, 31